J. Vis. Commun. Image R. 20 (2009) 1–8

Contents lists available at ScienceDirect

J. Vis. Commun. Image R.

journal homepage: www.elsevier.com/locate/jvci

2D motion aided sampling and reconstruction

Amiram Allouche [a], Arie Feuer [b,*]

[a] Surf Communications Solution Ltd., Yokne'am 20692, Israel
[b] Department of Electrical Engineering, Technion—Israel Institute of Technology, Haifa 32000, Israel

ARTICLE INFO

Article history:
Received 12 March 2007
Accepted 21 September 2008
Available online 2 October 2008

Keywords:
Super-resolution
Multi-dimensional
Nonuniform sampling
Multi-frame
Induced motion
Generalized sampling expansion (GSE)

ABSTRACT

In this paper we consider the problem of generating data which is sufficient for super resolution reconstruction. The method considered here is by inducing motion on the (low resolution) image acquisition device which then generates a number of low resolution images – this is the data we use for the super resolution reconstruction. Our main concern is in investigating a number of motion types and providing the conditions which will guarantee the feasibility of the super resolution reconstruction from data available.

1. Introduction

All digital acquisition devices have sensor arrays of finite spatial resolutions. As a result, the spatial details which can be captured using these devices are limited. While current resolutions get closer and closer to the resolutions of the traditional analog devices (which use film) in many instances, users would like to be able to capture details beyond the resolution constraints of their particular devices. A way to accomplish that, which attracted the interest of many researchers, is the "multi-frame Super Resolution". The term "muti-frame" is used to distinguish this method from various attempts to generate the high resolution frame from a single data frame. The latter are, typically, not considered "true" super resolution methods. Hence, in the sequel, when we refer to Super-Resolution (SR) it is the "multi-frame" we have in mind.

The basic idea in super-resolution is to use the device to generate a set of frames of, possibly, unsatisfactory resolution each, containing the same scene. Then, attempt to combine the information from this set of frames to generate a high resolution frame with all the desired spatial details – a SR frame. A large number of results describing different methods of generating the super-resolution frame have been published in the literature [1–11], just to name a few. More references can be found in survey papers such as [12]. Clearly, in order for these methods to work one need to guarantee that the set of data frames does indeed contain the information required in order to be able to generate the super-resolution frame. While many of the above SR reconstruction methods depend on some type of prior information of the SR image (such as smoothness, etc.) we make no such assumptions here.

The set up we consider here is a low resolution digital image acquisition device which is being moved while registering a sequence of (low resolution) images. The emphasis in this work is not on the actual SR reconstruction algorithm but rather, on the conditions which guarantee its feasibility from the available data set. We assume in the sequel that the data sampling pattern (as set by the device sensor array) and the desired resolution of the SR image are given. Hence, the design degrees of freedom are: type of device motion, its parameters (velocity or acceleration) and the temporal sampling interval. We develop the conditions on these parameters which will make the SR reconstruction possible.

2. Mathematical preliminaries and problem description

In the sequel we rely heavily on basic concepts from number theory and refer the reader unfamiliar with some of the basic notation to [19] or similar book. We will further need the following definitions:

Definition 1. If $Q \in \mathbb{N}$, then a *residue system* modulo Q is the set of all integers that are congruent to a fixed integer m modulo Q, denoted $\bar{m}$.

Definition 2. For $a, b, x \in \mathbb{Z}$ and $Q \in \mathbb{N}$ the relationship $ax \equiv b(\text{mod}\, Q)$ is called *linear congruence*.

* Corresponding author.
E-mail addresses: Amirama@Surf-com.com (A. Allouche), feuer@ee.technion.ac.il (A. Feuer).

1047-3203/$ - see front matter © 2008 Elsevier Inc. All rights reserved.
doi:10.1016/j.jvcir.2008.09.005

In the sequel we denote vectors by bold lower case and by $\hat{f}$, as is the standard in the literature, the Fourier transform of f.

Let $I_o(\mathbf{x}), \mathbf{x} \in \mathbb{R}^2$ be the image projected by the device optics on the sensor array and let $\mathcal{LAT}(S) = \{S\mathbf{k} : \mathbf{k} \in \mathbb{Z}^2\}$ denote the sensor array sampling pattern (lattice) corresponding to the matrix $S \in \mathbb{R}^{2\times2}$. While results for general lattices can be derived, for the sake of simplicity we restrict ourselves to the rectangular one where

$$S = \begin{bmatrix} \Delta x_1 & 0 \\ 0 & \Delta x_2 \end{bmatrix} \tag{1}$$

We assume ideal sampling hence, the data generated by the sensor array is given by $\{I_o(S\mathbf{k}) : \mathbf{k} \in \mathbb{Z}^2\}$. The device is now moved relative to the scene in a plane parallel to the scene. The resulting projected scene is then given by

$$I(\mathbf{x}, t) = I_o(\mathbf{x} - \mathbf{f}(t)) \tag{2}$$

where the vector $\mathbf{f}(t) \in \mathbb{R}^2$ represents the relative motion between the scene and the sensors. At this point we only assume,w.l.o.g., that $\mathbf{f}(0) = \mathbf{0}$. This time varying scene, $I(\mathbf{x}, t)$, is now sampled both temporally (with sampling interval Δt) and spatially on the lattice $\mathcal{LAT}(S)$. This way we get a sequence of sampled data frames $\{I_o(S\mathbf{k} - \mathbf{f}(n\Delta t)) : \mathbf{k} \in \mathbb{Z}^2, n \in \mathbb{Z}\}$. *We wish to find conditions under which $I_o(\mathbf{x})$ can be reconstructed from this data set.* Obviously, once $I_o(\mathbf{x})$ is reconstructed it can be re-sampled to any desired spatial (super) resolution.

We introduce next some additional notation. Let

$$\mathbf{g}(n) \triangleq \left\lceil S^{-1}\mathbf{f}(n\Delta t) \right\rceil - S^{-1}\mathbf{f}(n\Delta t) \tag{3}$$

where $\lceil \mathbf{f} \rceil = (\, \lceil f_1 \rceil s \quad \lceil f_2 \rceil \,)^T$ and $\lceil f \rceil = \min_{l \in \mathbb{Z}}\{l \geqslant f\}$,

$$\overline{n_\mathbf{g}} = \{m \in \mathbb{Z} : \mathbf{g}(m) = \mathbf{g}(n)\} \tag{4}$$

$$\mathcal{N}_\mathbf{g} = \left\{ \{n_m\}_{m=1}^M : \overline{(n_{m_1})_\mathbf{g}} \cap \overline{(n_{m_2})_\mathbf{g}} = \emptyset \text{ for } m_1 \neq m_2 \right. \\ \left. \text{and} \quad \bigcup_{m=1}^M \overline{(n_m)_\mathbf{g}} = \mathbb{Z} \right\} \tag{5}$$

and

$$\mathbf{x}_i = S\mathbf{g}(n_i) \text{ such that } n_i \in \mathcal{N}_\mathbf{g} \tag{6}$$

We note that the set $\mathcal{N}_\mathbf{g}$ is not unique, however, all such sets have the same number of members in them, say M. Hence, without loss of generality we choose $n_1 = 0 \in \mathcal{N}_\mathbf{g}$ and then $\mathbf{x}_1 = \mathbf{0}$.

With the above notation, we can rewrite the data set as

$$\begin{aligned} &\{I_o(S\mathbf{k} - \mathbf{f}(n\Delta t)) : \mathbf{k} \in \mathbb{Z}^2, n \in \mathbb{Z}\} \\ &\quad = \{I_o(S\mathbf{k} + S\mathbf{g}(n)) : \mathbf{k} \in \mathbb{Z}^2, n \in \mathbb{Z}\} \\ &\quad = \{I_o(S\mathbf{k} + S\mathbf{g}(n_i)) : \mathbf{k} \in \mathbb{Z}^2, n_i \in \mathcal{N}_\mathbf{g}\} \\ &\quad = \{I_o(S\mathbf{k} + \mathbf{x}_i) : \mathbf{k} \in \mathbb{Z}^2, i = 1, \ldots, M\} \end{aligned} \tag{7}$$

This is readily recognized as recurrent sampling of the image $I_o(\mathbf{x})$ (see e.g. [13]).

In the sequel we make extensive use of the multi-dimensional version of the generalized sampling expansion (GSE) results (see e.g.[14,15]). For the benefit of the reader we formally restate a general form of this result below:

Theorem 3. *Let $I_o(\mathbf{x})$, $\mathbf{x} \in \mathbb{R}^2$ be a bandlimited signal which is passed through a bank of M LTI filters $\{\hat{h}_i(\omega)\}_{i=1}^M$ as in Fig. 1, to generate the signals $I_i(\mathbf{x})$. Namely, $\widehat{I}_i(\omega) = \hat{h}_i(\omega)\widehat{I}_o(\omega)$. Then, a necessary and sufficient condition that $I_o(\mathbf{x})$ can be reconstructed from $\{I_i(S\mathbf{k}) : \mathbf{k} \in \mathbb{Z}^2\}_{i=1}^M$ is that the matrix*

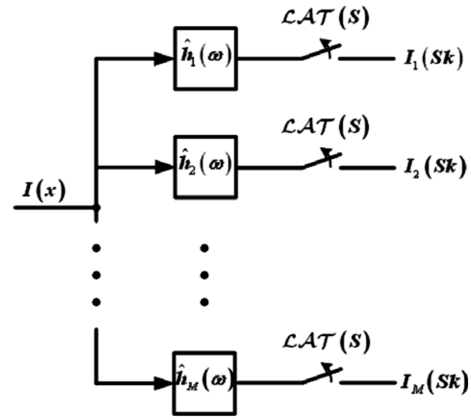

Fig. 1. The generalized sampling expansion (GSE) configuration.

$$H(\omega) = \begin{bmatrix} \hat{h}_1(\omega + \mathbf{c}_1) & \hat{h}_2(\omega + \mathbf{c}_1) & \cdots & \hat{h}_M(\omega + \mathbf{c}_1) \\ \hat{h}_1(\omega + \mathbf{c}_2) & \hat{h}_2(\omega + \mathbf{c}_2) & \cdots & \hat{h}_M(\omega + \mathbf{c}_2) \\ \vdots & \vdots & \ddots & \vdots \\ \hat{h}_1(\omega + \mathbf{c}_N) & \hat{h}_2(\omega + \mathbf{c}_N) & \cdots & \hat{h}_M(\omega + \mathbf{c}_N) \end{bmatrix} \in \mathbb{C}^{N\times M} \tag{8}$$

is full row rank for all $\omega \in \mathcal{UC}(2\pi S^{-T})$ (by $\mathcal{UC}(2\pi S^{-T})$ we denote a unit cell in the lattice $\mathcal{LAT}(2\pi S^{-T})$), where $\{\mathbf{c}_l\}_{l=1}^N \subset \mathcal{LAT}(2\pi S^{-T})$ are such that

$$supp(\widehat{I}_o(\omega)) \subseteq \bigcup_{l=1}^N \left\{ \mathcal{UC}(2\pi S^{-T}) + \mathbf{c}_l \right\} \tag{9}$$

Under these conditions, the reconstruction formula is given by

$$I_o(\mathbf{x}) = \sum_{i=1}^M \sum_{\mathbf{k}\in\mathbb{Z}^2} I_i(S\mathbf{k})\varphi_i(\mathbf{x} - S\mathbf{k}) \tag{10}$$

where

$$\varphi_i(\mathbf{x}) = \frac{|\det(S)|}{(2\pi)^2} \int_{\mathcal{UC}(2\pi S^{-T})} \Phi_i(\omega, \mathbf{x})\, e^{j\omega^T\mathbf{x}}\, d\omega \tag{11}$$

and $\Phi_n(\omega, \mathbf{x})$ are the solutions of the equation

$$H(\omega) \begin{bmatrix} \Phi_1(\omega, \mathbf{x}) \\ \Phi_2(\omega, \mathbf{x}) \\ \vdots \\ \Phi_M(\omega, \mathbf{x}) \end{bmatrix} = \begin{bmatrix} e^{j\mathbf{c}_1^T\mathbf{x}} \\ e^{j\mathbf{c}_2^T\mathbf{x}} \\ \vdots \\ e^{j\mathbf{c}_N^T\mathbf{x}} \end{bmatrix} \tag{12}$$

if they exist.

To see the connection to our problem, let the filters above be chosen as shifts, namely

$$\hat{h}_i(\omega) = e^{j\omega^T\mathbf{x}_i} \tag{13}$$

where $\mathbf{x}_i$ is as in (6). Then, we readily observe that $\{I_o(S\mathbf{k} + \mathbf{x}_i) : \mathbf{k} \in \mathbb{Z}^2, i = 1, \ldots, M\} = \{I_i(S\mathbf{k}) : \mathbf{k} \in \mathbb{Z}^2, i = 1, \ldots, M\}$, hence Theorem 3 can be directly applied to our reconstruction problem. Specifically, our ability to reconstruct the desired signal depends on whether the matrix $H(\omega) \in \mathbb{C}^{N\times M}$ is indeed full row rank so that Eq. (12) has a solution. We note that by assuming that $I_o(\mathbf{x})$ is bandlimited the existence of the set $\{\mathbf{c}_l\}_{l=1}^N \subset \mathcal{LAT}(2\pi S^{-T})$ such that (9) is satisfied, is guaranteed. This is true for any bandlimited image and any unit cell of the reciprocal lattice. However, to further simplify our discussion we choose the unit cell

$$\mathcal{UC}(2\pi S^{-T}) = \left\{ \omega : -\frac{\pi N_j}{\Delta x_j} \leqslant \omega_j < \frac{\pi(2 - N_j)}{\Delta x_j}, \quad j = 1, 2 \right\} \tag{14}$$

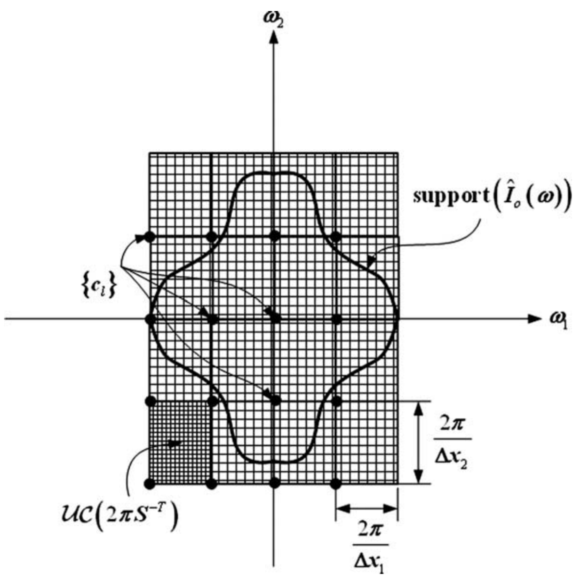

Fig. 2. Signal spectral support and its covering.

Then, for appropriate N_j we have

$$\text{supp }(\widehat{I}_o(\boldsymbol{\omega})) \subseteq \left\{\boldsymbol{\omega} : -\frac{\pi N_j}{\Delta x_j} \leqslant \omega_j < \frac{\pi N_j}{\Delta x_j}, \quad j = 1,2\right\} \tag{15}$$

which means that

$$\mathbf{c}_l = 2\pi S^{-T}\mathbf{m}_l \tag{16}$$

and $m_{l,j} \in \{0, 1, \ldots, N_j - 1\}$. This is demonstrated in Fig. 2. Note that the number of shifted unit cells required is $N = N_1N_2$.

Using (13) we have

$$\hat{h}_i(\boldsymbol{\omega} + \mathbf{c}_l) = e^{j(\boldsymbol{\omega}+\mathbf{c}_l)^T\mathbf{x}_i} = e^{j\boldsymbol{\omega}^T\mathbf{x}_i}e^{j\mathbf{c}_l^T\mathbf{x}_i}$$

hence, the matrix $H(\boldsymbol{\omega})$ can be rewritten as

$$H(\boldsymbol{\omega}) = \mathscr{H}\begin{bmatrix} e^{j\boldsymbol{\omega}^T\mathbf{x}_1} & 0 & \cdots & 0 \\ 0 & e^{j\boldsymbol{\omega}^T\mathbf{x}_2} & \cdots & 0 \\ \vdots & \vdots & \ddots & \vdots \\ 0 & 0 & \cdots & e^{j\boldsymbol{\omega}^T\mathbf{x}_M} \end{bmatrix}$$

where

$$\mathscr{H} = \begin{bmatrix} e^{j\mathbf{c}_1^T\mathbf{x}_1} & e^{j\mathbf{c}_1^T\mathbf{x}_2} & \cdots & e^{j\mathbf{c}_1^T\mathbf{x}_M} \\ e^{j\mathbf{c}_2^T\mathbf{x}_1} & e^{j\mathbf{c}_2^T\mathbf{x}_2} & \cdots & e^{j\mathbf{c}_2^T\mathbf{x}_M} \\ \vdots & \vdots & \ddots & \vdots \\ e^{j\mathbf{c}_N^T\mathbf{x}_1} & e^{j\mathbf{c}_N^T\mathbf{x}_2} & \cdots & e^{j\mathbf{c}_N^T\mathbf{x}_M} \end{bmatrix} \tag{17}$$

Clearly then, $H(\boldsymbol{\omega})$ is full row rank if and only if $\mathscr{H}$ is. Hence, from now on we will concentrate on the conditions which make the matrix $\mathscr{H}$ full row rank. The first and immediate necessary condition is $N \leqslant M$ but, for simplicity we will assume.

$$N = M \tag{18}$$

Remark 4. The functions defined in (11), $\varphi_i(\mathbf{x})$, can be viewed as impulse responses of filters so that the reconstruction formula (10), can be implemented as a filter bank. While, as stated above, we assume (18) in the sequel, reconstruction is possible for $N < M$ as long as $\mathscr{H}$ is full rank. In this case the functions (filters) are not unique and one can incorporate robustness criteria in the process of calculating $\varphi_i(\mathbf{x})$ resulting in a more robust reconstruction. A more detailed discussion on this issue is beyond the scope of this paper, however, in our simulations we did implement a robust reconstruction whenever we had $N < M$.

3. General motion along a straight line

While for 1D signals (18) is a sufficient condition as well (see e.g. [16]), going into two or higher dimensional signals makes the problem considerably more complex. We restrict ourselves here, to the 2D case only and to *motion along a straight line.*

In that case we have

$$\mathbf{f}(t) = f(t)\boldsymbol{\alpha}_o \tag{19}$$

where the constant vector $\boldsymbol{\alpha}_o$ is the direction of the motion and $f(t)$ is the type of motion in that direction. Substituting (19) in (3) we get

$$\begin{aligned}\mathbf{g}(n_i) &= \left\lceil S^{-1}\mathbf{f}(n_i\Delta t)\right\rceil - S^{-1}\mathbf{f}(n_i\Delta t) \\ &= \left\lceil fn_i\Delta t)S^{-1}\boldsymbol{\alpha}_o\right\rceil - f(n_i\Delta t)S^{-1}\boldsymbol{\alpha}_o \end{aligned} \tag{20}$$

In the sequel we will assume that $\boldsymbol{\alpha}_o \in \mathscr{LAT}(S)$ which means that $S^{-1}\boldsymbol{\alpha}_o = \boldsymbol{\alpha} = (\,\alpha_1 \quad \alpha_2\,)^T \in \mathbb{Z}^2$ with α_1 and α_2 *coprime*. We note that this assumption is not very restrictive as every slope can be approximated to any desired degree by a rational slope (modulo practical constraints) constrained by. We further assume that $f(n\Delta t)$, for every $n \in \mathbb{Z}$, is a rational number of the form

$$f(n\Delta t) = \frac{b(n)}{Q} \tag{21}$$

where $Q, b(n) \in \mathbb{Z}$. Then we can prove the following helpful result:

Lemma 5. *For every $n \in \mathbb{Z}$ there exists a unique $n_i \in \mathscr{N}_\mathbf{g}$ such that $b(n) \equiv b(n_i)(mod\, Q)$.*

Proof. Suppose $\mathbf{g}(n) = \mathbf{g}(n_i)$ for $n, n_i \in \mathbb{Z}$. Then

$$\left\lceil \frac{b(n)}{Q}\begin{bmatrix}\alpha_1\\ \alpha_2\end{bmatrix}\right\rceil - \frac{b(n)}{Q}\begin{bmatrix}\alpha_1\\ \alpha_2\end{bmatrix} = \left\lceil \frac{b(n_i)}{Q}\begin{bmatrix}\alpha_1\\ \alpha_2\end{bmatrix}\right\rceil - \frac{b(n_i)}{Q}\begin{bmatrix}\alpha_1\\ \alpha_2\end{bmatrix}$$

so that

$$\frac{b(n_i) - b(n)}{Q}\begin{bmatrix}\alpha_1\\ \alpha_2\end{bmatrix} \in \mathbb{Z}^2$$

and as α_1 and α_2 are coprime, we must have $b(n) \equiv b(n_i)(\text{mod}\, Q)$. Suppose now $b(n) \equiv b(n_i)(\text{mod}\, Q)$ for $n, n_i \in \mathbb{Z}$. Namely, $b(n) = b(n_i) + qQ$ for some $q \in \mathbb{Z}$. Then

$$\begin{aligned}\mathbf{g}(n) &= \left\lceil \frac{b(n)}{Q}\begin{bmatrix}\alpha_1\\ \alpha_2\end{bmatrix}\right\rceil - \frac{b(n)}{Q}\begin{bmatrix}\alpha_1\\ \alpha_2\end{bmatrix} = \left\lceil \frac{b(n_i) + qQ}{Q}\begin{bmatrix}\alpha_1\\ \alpha_2\end{bmatrix}\right\rceil \\ &\quad - \frac{b(n_i) + qQ}{Q}\begin{bmatrix}\alpha_1\\ \alpha_2\end{bmatrix} = \left\lceil \frac{b(n_i)}{Q}\begin{bmatrix}\alpha_1\\ \alpha_2\end{bmatrix}\right\rceil - \frac{b(n_i)}{Q}\begin{bmatrix}\alpha_1\\ \alpha_2\end{bmatrix} = \mathbf{g}(n_i)\end{aligned}$$

We have shown that $\mathbf{g}(n) = \mathbf{g}(n_i)$ if and only if $b(n) \equiv b(n_i)(\text{mod}\, Q)$. As, by the definition of $\mathscr{N}_\mathbf{g}$, for every $n \in \mathbb{Z}$ there exists a unique $n_i \in \mathscr{N}_\mathbf{g}$ such that $\mathbf{g}(n) = \mathbf{g}(n_i)$ the proof is completed. □

An important consequence of Lemma 5 is the following inequality:

$$M \leqslant Q \tag{22}$$

Let us now view the (l,i)th entry of the matrix $\mathscr{H}$. By (17), (20) and (21) we have

$$\mathscr{H}_{l,i} = e^{j\mathbf{c}_l^T\mathbf{x}_i} = e^{j2\pi\mathbf{m}_l^T\mathbf{g}(n_i)} = e^{-j\frac{2\pi}{Q}(\alpha_1 m_{l,1} + \alpha_2 m_{l,2})b(n_i)} = \varepsilon^{\tilde{m}_l}b(n_i) \tag{23}$$

where $\varepsilon = e^{-j\frac{2\pi}{Q}}$ and $\tilde{m}_l = \alpha_1 m_{l,1} + \alpha_2 m_{l,2}$.

A matrix with entries as in (23) is commonly referred to as 'generalized Vandermonde' matrix. General conditions for its nonsingularity, to the best of our knowledge, do not exist in the literature. For the case where Q *is a prime number* we have the following result (see [17]).

Theorem 6. *Let ε be a Qth root of 1 over the complex field $\mathbb{C}$. The square matrix, the (l,i)th entry of which is $\varepsilon^{\tilde{m}_l b(n_i)}$, is nonsingular for a prime Q if and only if the integers $\{\tilde{m}_l\}_{l=1}^{N}$ are pairwise incongruent modulo Q and so are the integers $\{b(n_i)\}_{i=1}^{M}$.*

Remark 7. The result in [17] states and proves only sufficiency. However, necessity is readily observed since if any two integers $\tilde{m}_{l_1}, \tilde{m}_{l_2}$ are congruent modulo Q, the two corresponding two rows (columns) in the matrix are identical and singularity of the matrix follows.

As by Lemma 5 the integers $\{b(n_i)\}_{i=1}^{M}$ are pairwise incongruent modulo Q we will concentrate on the conditions which will make the set $\{\tilde{m}_l\}_{l=1}^{N}$ pairwise incongruent modulo Q. For given integers N_1, N_2 and Q this set of integers depends on the choice of motion direction. Namely, on the choice of the integers α_1, α_2. So, let us denote

$$\mathscr{M}(\alpha_1,\alpha_2) = \{\tilde{m} = \alpha_1 m_1 + \alpha_2 m_2 : 0 \leqslant m_1 \leqslant N_1 - 1, 0 \leqslant m_2 \leqslant N_2 - 1\} \quad (24)$$

and we establish the following result:

Lemma 8. *For the given $N_1, N_2 \in \mathbb{N}$ and Q a prime number consider the set $\mathscr{X}$ of all the (unique mod Q) solutions of the linear congruences $m_1 x \equiv m_2 (\mathrm{mod}\, Q)$ where $(m_1, m_2) \neq (0,0)$, $|m_1| \leqslant N_1 - 1$ and $|m_2| \leqslant N_2 - 1$. Then, there exist α_1, α_2 such that all integers in $\mathscr{M}(\alpha_1, \alpha_2)$ are pairwise incongruent modulo Q if and only if*

$$|\mathscr{X}| < Q \quad (25)$$

(by $|\mathscr{X}|$ we denote the cardinality of the set $\mathscr{X}$).

Proof. The proof is given in Appendix A. □

We can now state our result for general motion along a straight line:

Theorem 9. *Suppose a digital image acquisition device with a spatial sampling of the form $\mathscr{LAT}(S) = \{S\mathbf{k} : \mathbf{k} \in \mathbb{Z}^2\}$, S as in (1), is moving relative to a scene in a motion given in (19). A sequence of data frames is being generated at intervals Δt so that (21) holds for some prime Q. Assuming the scene is a bandlimited image satisfying (14) the image of the scene can be reconstructed to any desired resolution (modulo practical constraints) from the available data if (18) and (25) are satisfied.*

Proof. The proof follows directly from Theorems 3 and 6 and Lemmas 5 and 8. □

Remark 10. We note that for every $x \in \mathscr{X}$, $Q - x \in \mathscr{X}$. Hence, to generate the set $\mathscr{X}$ one can find the solutions of the linear congruences $m_1 x \equiv m_2 (\mathrm{mod}\, Q)$ for $1 \leqslant m_1 \leqslant N_1 - 1$ and $1 \leqslant m_2 \leqslant N_2 - 1$ only and for each, add also $Q - x$ to the set. To demonstrate these calculations, let us consider two cases: $(N_1, N_2, Q) = (3, 5, 11)$ and $(N_1, N_2, Q) = (3, 5, 17)$. For the first we get $\mathscr{X} = \{1, 2, \ldots, 11\}$ while for the second case $\mathscr{X} = \{1, 2, 4, 5, 6, 8, 9, 11, 12, 13, 15, 16, 17\}$ (it *does not contain* the integers $\{3, 7, 10, 14\}$).

Remark 11. An immediate consequence of Theorem 6 is that in some cases there are no directions along which the motion could generate the necessary data for reconstruction while in other cases, such directions exist and can be calculated. For the two cases mentioned in Remark 10 we have that for $(N_1, N_2, Q) = (3, 5, 11)$ reconstruction is impossible for any motion in any direction while for $(N_1, N_2, Q) = (3, 5, 17)$ reconstruction will be possible for motion along the family of directions $(y\alpha_2 + 17k, \alpha_2 + 17l)$ where $k, l \in \mathbb{Z}$ and $y \in \{3, 7, 10, 14\}$.

4. Specific motions along a straight line

In this section we consider a number of specific motions along a straight line. Theorem 9 establishes the general framework of the types of motions we consider. For each motion we establish the relationship between the temporal sampling interval, motion parameters and the values of M, $b(n)$, and Q in (18) and (21). Armed with this, one can readily modify the motion so that (18) and (25) are satisfied. Once these conditions are satisfied, as stated in Theorem 9, the data generated is sufficient for the SR reconstruction.

4.1. Constant velocity

We start with the simplest type of motion, constant velocity. This type of motion has been investigated before (see e.g. [18] and [8]). In this case we have $f(t) = Vt$. Choose $V\Delta t = \frac{R_1}{Q_1}$, $R_1, Q_1 \in \mathbb{N}$ such that gcd $(R_1, Q_1) = 1$ and Q_1 is prime. Then we have $M = Q_1$ (see [16]) and $\frac{b(n)}{Q} = \frac{nR_1}{Q_1}$.

Remark 12. While the approach in [8] is quite different from the one used here, it can be shown that the results for the constant speed case are similar. Furthermore, the best direction as stated in [8] translates here to the direction for which the reconstruction process is the most robust. Namely, the choice for which the condition number of the resulting matrix $\mathscr{H}$ is the smallest.

4.2. Periodic motion

Periodic motions are, in our opinion, the most interesting from a practical point of view. An immediate observation for a general periodic motion of period T and temporal sampling rate Δt, is that if $\frac{\Delta t}{T} = \frac{R_1}{Q_1}$ is a rational number then

$$f(n\Delta t) = f(n\Delta t + R_1 T) = f(n\Delta t + Q_1 \Delta t) = f((n + Q_1)\Delta t)$$

which means that that

$$M \leqslant Q_1 \quad (26)$$

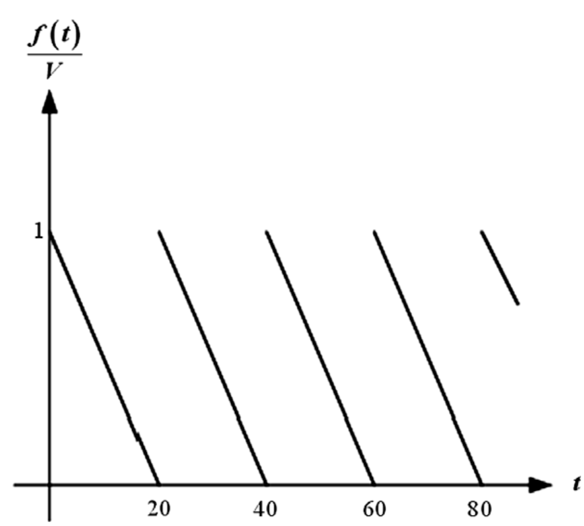

Fig. 3. Sawtooth motion ($T = 20$).

We consider now two types of periodic motions: Sawtooth and triangular.

4.2.1. Sawtooth motion

Consider the motion $f(t)$ given by

$$f(t) = V\left(\left\lceil \frac{t}{T}\right\rceil - \frac{t}{T}\right) \tag{27}$$

(see Fig. 3). The results we have for this motion are summarized in the following claim:

Claim 13. *Let $f(t)$ be as in (27) We assume $\frac{\Delta t}{T} = \frac{R_1}{Q_1}$ and $V = \frac{R_2}{Q_2}$ where $R_i, Q_i \in \mathbb{N}$, Q_2 is prime, $\gcd(R_1, Q_1) = 1$ and Δt is the temporal sampling interval. Then, if $R_2 = R_3 Q_1$ (21) is satisfied with $Q = Q_2$*

$$b(n) = R_3\left(Q_1\left\lceil \frac{nR_1}{Q_1}\right\rceil - nR_1\right) \tag{28}$$

and

$$M = \min(Q_1, Q_2) \tag{29}$$

Proof. Substituting $t = n\Delta t$ in (27) leads to

$$f(n\Delta t) = \frac{Q_1 R_3}{Q_2}\left(\left\lceil \frac{nR_1}{Q_1}\right\rceil - \frac{nR_1}{Q_1}\right)$$

and using (28) we get

$$f(n\Delta t) = \frac{b(n)}{Q_2}$$

which has the form of (21) with $Q = Q_2$. To prove (29) we first recall from the proof of Lemma 5 that $\mathbf{g}(n) = \mathbf{g}(n_i) \iff b(n) \equiv b(n_i)(\mathrm{mod}\, Q_2)$. As $\gcd(R_1, Q_1) = 1$ it follows that

$$b(n) = b(n_i) \iff \left(\left\lceil \frac{nR_1}{Q_1}\right\rceil Q_1 - nR_1\right) = \left(\left\lceil \frac{n_i R_1}{Q_1}\right\rceil Q_1 - n_i R_1\right) \iff n \equiv n_i\ (\mathrm{mod}\, Q_1)$$

so that $\{b(n)\}_{n=0}^{Q_1-1}$ is a set of distinct integers. However, as we know that at most Q_2 integers can be distinct $(\mathrm{mod}\, Q_2)$, (29) follows. □

4.2.2. Triangular wave motion

Consider the motion $f(t)$ given by

$$f(t) = V\left|\left\lceil \frac{t}{T} - \frac{1}{2}\right\rceil - \frac{t}{T}\right| \tag{30}$$

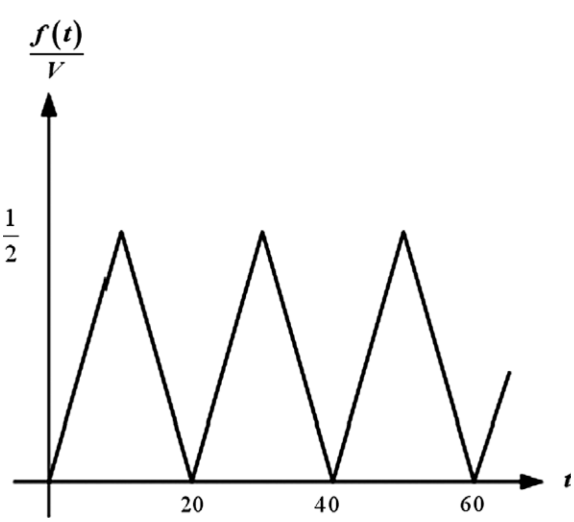

Fig. 4. Triangular wave motion ($T = 20$).

(see Fig. 4). The results we have for this motion are summarized in the following claim:

Claim 14. *Let $f(t)$ be as in (30) We assume $\frac{\Delta t}{T} = \frac{R_1}{Q_1}$ and $V = \frac{R_2}{Q_2}$ where $R_i, Q_i \in \mathbb{N}$, Q_2 is prime, $\gcd(R_1, Q_1) = 1$ and Δt is the temporal sampling interval. Then, if $R_2 = R_3 Q_1$ (21) is satisfied with $Q = Q_2$*

$$b(n) = R_2\left|Q_1\left\lceil \frac{nR_1}{Q_1} - \frac{1}{2}\right\rceil - nR_1\right| \tag{31}$$

and

$$M = \min\left(\left\lfloor \frac{Q_1}{2}\right\rfloor + 1, Q_2\right) \tag{32}$$

Proof. By substitution we readily get the format of (21) with $Q = Q_2$ and (31). Since $\gcd(R_1, Q_1) = 1$

$$\begin{aligned} b(n) = b(n_i) &\iff \left|\left\lceil \frac{nR_1}{Q_1} - \frac{1}{2}\right\rceil Q_1 - nR_1\right| \\ &= \left|\left\lceil \frac{n_i R_1}{Q_1} - \frac{1}{2}\right\rceil Q_1 - n_i R_1\right| \iff n \equiv n_i(\mathrm{mod}\, Q_1) \\ \text{or } n &\equiv -n_i(\mathrm{mod}\, Q_1) \end{aligned} \tag{33}$$

therefore $\{b(n)\}_{n=0}^{\lfloor \frac{Q_1}{2}\rfloor}$ is a set of distinct integers. Again, as we know that at most Q_2 integers can be pair wise incongruent $(\mathrm{mod}\, Q_2)$, (32) follows. □

4.3. Constant acceleration

This motion has been discussed in [6] so, while not very practical, we do present the results for this motion as well. Let $f(t)$ be given by

$$f(t) = at^2 \tag{34}$$

Then we can state the following result:

Claim 15. *Let $f(t)$ be as in (34). We assume $a(\Delta t)^2 = \frac{R_1}{Q_1}$ where Q_1 is prime and $\gcd(R_1, Q_1) = 1$. Then (21) is satisfied with $Q = Q_1$*

$$b(n) = R_1 n^2 \tag{35}$$

and

$$M = \left\lfloor \frac{Q_1}{2}\right\rfloor + 1 \tag{36}$$

Proof. By substitution we readily get the format of (21) with $Q = Q_1$ and (35). Furthermore, since $\gcd(R_1, Q_1) = 1$ we have

$$\begin{aligned} &b(n) \equiv b(n_i)(\mathrm{mod}\, Q1) \iff n^2 \equiv n_i^2(\mathrm{mod}\, Q_1) \iff n \equiv n_i(\mathrm{mod}\, Q_1) \\ &\text{or} \quad n \equiv -n_i(\mathrm{mod}\, Q_1) \end{aligned} \tag{37}$$

therefore $\{b(n)\}_{n=0}^{\lfloor \frac{Q_1}{2}\rfloor}$ is a set of pair wise incongruent integers $(\mathrm{mod}\, Q_1)$ and (36) follows. □

5. Simulation results

To demonstrate the validity of our results we have carried out extensive simulations, some of which we will present here. In our experiments we assume we do have the true super resolution image and we compare it, in each case, to the reconstructed one. As an objective criteria for the quality of the reconstructed image we use peak signal to noise ratio (PSNR) – a commonly used measure (see e.g. [20]) defined by

$$\mathrm{PSNR} = 10\log_{10}\left(\frac{255^2}{\frac{1}{K_x K_y}\sum_{k=0}^{K_x-1}\sum_{l=0}^{K_y-1}(I_o() - I_{\mathrm{rec}}())^2}\right) \tag{38}$$

where I_o and I_{rec} are the true and reconstructed super resolution images respectively, each of $K_x \times K_y$ pixels. We present two sets of experiments. One on artificial images and the other on real images.

5.1. Artificial images

The image we created here is defined by

$$I_o(\mathbf{x}) = \frac{255}{2}\left[1 + \sin\left(\omega_1^T \mathbf{x}\right) + \sin\left(\omega_2^T \mathbf{x}\right)\right]$$

where $\omega_1^T = 2\pi[0.39, 0.42]$ and $\omega_2^T = 2\pi[0.29, 0.39]$. Choosing $\Delta x_1 = \Delta x_2 = 2$ we get $N_1 = N_2 = 2$. We considered a finite section of the image $[0, 128\Delta x_1] \times [0, 128\Delta x_2]$ and used as temporal sampling $\Delta t = 2$ generating, in each case, 40 frames. Table 1 summarizes the results of our experiments. We wish to point out that in all the experiments, the calculated M was identical to the result in the experiment. In the first three experiments we have $M = N = N_1 N_2 = 4$. Hence, the 'does not apply' in the column '$N < M$' for these experiments. For the other two experiments, where indeed the resulting M is greater than $N = 4$, we did the reconstruction in two ways represented in the two distinct columns. In one we just use N sample points resulting in a non-singular reconstruction matrix, while in the other, we used all the M distinct data points resulting in a full row rank matrix and in a least square solution to the reconstruction functions. Clearly, the latter results in a much improved performance in both experiments (4) and (5). Also note that in experiment (1), the direction of motion is such that $\mathscr{M}(3,4) = \{0, 3, 4, 7\}$ and $Q = 7$, so that $7 \equiv 0 (\text{mod}\, 7)$ and by Theorem 6 the resulting matrix should be singular – the simulation confirmed this result as stated in Table 1.

Table 2
Robustness Testing Results

Experiment No.	Motion type	Motion parameters	Noise	PSNR (dB)
1	Triangular	$V = \frac{132}{31}; T = 33; \boldsymbol{\alpha} = \begin{bmatrix} 2 \\ 7 \end{bmatrix}$	No	38
2	Sawtooth	$V = \frac{68}{31}; T = 33; \boldsymbol{\alpha} = \begin{bmatrix} 3 \\ 7 \end{bmatrix}$	Yes	30.2

5.2. Real images

For our experiments on real data we have used the images of Lena and Barbara (see Fig. 5 for the original image – 512×512 pixels). Motion was applied to these image, they were down sampled to $\Delta x_1 = \Delta x_2 = 4$ and the reconstruction was to the original images, namely, $N_1 = N_2 = 4$. We used $\Delta t = 1$ to generate 40 frames of low resolution data. Just for perspective, the ability to increase resolution by a factor of 16 as we did here, could take a sequence of 2 mega pixels frames (typical in inexpensive digital cameras today) and get an image of 32 mega pixels with all the details. Or, another attractive use could be to enable a $\times 4$ *true* digital zoom.

In these experiments we have also tested the robustness to noise and to errors in motion parameters and their effects on the reconstruction. A small sample of the results is presented in Table 2 The reconstructed images are presented in Fig. 6. Note that we used different types of motion for each image and that in one case no noise was added while in the other we did add noise. The added noise was normalized so that for each low resolution data frame the resulting PSNR was 40 dB. Also observe the high frequency details in the Barbara image and how well did the reconstruction handle them.

Table 1
Simulation Experiment Results

Experiment No.	Experiment description	Motion parameters	PSNR (dB) for $N = M$	PSNR (dB) for $N < M$
1	Constant acceleration	$a = \frac{1}{7}; \boldsymbol{\alpha} = \begin{bmatrix} 3 \\ 4 \end{bmatrix}$	Singular matrix	Does not apply
2	Constant acceleration	$a = \frac{1}{7}; \boldsymbol{\alpha} = \begin{bmatrix} 3 \\ 5 \end{bmatrix}$	29.2	Does not apply
3	Constant acceleration	$a = \frac{3}{7}; \boldsymbol{\alpha} = \begin{bmatrix} 1 \\ 2 \end{bmatrix}$	30.4	Does not apply
4	Sawtooth	$V = \frac{132}{31}; T = 33; \boldsymbol{\alpha} = \begin{bmatrix} 3 \\ 7 \end{bmatrix}$	23.8	35.7
5	Triangular	$V = \frac{132}{31}; T = 33; \boldsymbol{\alpha} = \begin{bmatrix} 3 \\ 7 \end{bmatrix}$	27	35

Fig. 5. Original images.

Fig. 6. Reconstructed images.

6. Conclusion

The problem we consider in this paper is that of generating sufficient data for super-resolution reconstruction (without the need for priors and regularizations). We have assumed that motion is induced on the data acquisition (low resolution) device and a sequence of (low resolution) frames is generated with a predetermined time interval (temporal sampling interval) between them. Our main concern in this paper has been choosing the motion and the temporal sampling so that a true super resolution reconstruction is feasible, without resorting to a variety of regularizations commonly used in the literature. We have concentrated here on deriving sufficient (and necessary) conditions on a variety of motions considered so that the resulting data are indeed sufficient for the reconstruction. Extensive experiments were carried out to test the validity of our analysis and a sample of the results is presented here. For the reconstruction itself we have used a filter bank structure resulting from the GSE ideas. There is no doubt that the reconstruction itself can be further improved by using more elaborate filter design methodologies.

Appendix A. Proof of Lemma 8

Proof. Suppose (25) holds. Namely, there exists an integer $1 \leqslant x_1 \leqslant Q-1$ such that

$$m_1 x_1 \ncong m_2 \ (\mathrm{mod}\, Q) \tag{A.1}$$

for all $(m_1, m_2) \neq (0,0)$, $|m_1| \leqslant N_1 - 1$ and $|m_2| \leqslant N_2 - 1$. Then, we claim that $\mathscr{M}(\alpha_2 x_1, \alpha_2)$ has the desired property for any $0 \neq \alpha_2 \in \mathbb{Z}$. Else, if $\tilde{m}_i \neq \tilde{m}_j \in \mathscr{M}(\alpha_2 x_1, \alpha_2)$ are congruent mod Q, we have, using (24),

$$\alpha_2(x_1 m_{i,1} + m_{i,2}) \equiv \alpha_2(x_1 m_{j,1} + m_{j,2}) (\mathrm{mod}\, Q)$$

or

$$(m_{i,1} - m_{j,1}) x_1 \equiv (m_{j,2} - m_{i,2}) (\mathrm{mod}\, Q)$$

which, as $(m_{i,1} - m_{j,1}, m_{j,2} - m_{i,2}) \neq (0,0)$, $|m_{i,1} - m_{j,1}| \leqslant N_1 - 1$ and $|m_{j,2} - m_{i,2}| \leqslant N_2 - 1$, contradicts (A.1).

Suppose now that $\mathscr{M}(\alpha_1, \alpha_2)$ has the desired property for some $\alpha_1, \alpha_2 \in \mathbb{Z}$. Namely,

$$\alpha_1 m_{i,1} + \alpha_2 m_{i,2} \ncong (\alpha_1 m_{j,1} + \alpha_2 m_{j,2}) \ (\mathrm{mod}\, Q)$$

or

$$\alpha_1(m_{i,1} - m_{j,1}) \ncong \alpha_2(m_{j,2} - m_{i,2}) \ (\mathrm{mod}\, Q) \tag{A.2}$$

for all $0 \leqslant m_{i,1}, m_{j,1} \leqslant N_1 - 1$ and $0 \leqslant m_{i,2}, m_{j,2} \leqslant N_2 - 1$ such that $(m_{i,1}, m_{i,2}) \neq (m_{j,1}, m_{j,2})$. Let x_1 be the unique solution of the linear congruence $\alpha_2 x \equiv \alpha_1 (\mathrm{mod}\, Q)$ such that $1 \leqslant x_1 \leqslant Q$. Then, by substituting into (A.2) we have

$$x_1(m_{i,1} - m_{j,1}) \ncong (m_{j,2} - m_{i,2}) \ (\mathrm{mod}\, Q)$$

for all $(m_{i,1} - m_{j,1}, m_{j,2} - m_{i,2}) \neq (0,0)$, $|m_{i,1} - m_{j,1}| \leqslant N_1 - 1$ and $|m_{j,2} - m_{i,2}| \leqslant N_2 - 1$. This means that $x_1 \notin \mathscr{X}$ and (3) follows, which completes the proof. □

References

[1] M. Elad, A fast super-resolution reconstruction algorithm for pure translational motion and common space-invariant blur, IEEE Transactions on Image Processing 10 (8) (2001) 1187–1193.
[2] M. Elad, A. Feuer, Restoration of a single super-resolution image from several blurred, noisy and under-sampled measured images, IEEE Transactions on Image Processing 6 (12) (1997) 1646–1658.
[3] M. Elad, A. Feuer, Super-resolution reconstruction of image sequences, IEEE Transactions on Pattern Analysis and Machine Intelligence 21 (9) (1999) 817–834.
[4] R.Y. Tsai, T.S. Huang, Multipleframe Image Restoration and Registration: Advances in Computer Vision and Image Processing, JAI Press Inc., 1984. pp. 317–339.
[5] M. Irani, S. Peleg, Motion analysis for image enhancement: resolution, occlusion, and transparency, Journal of Visual Communication and Image Representation 4 (4) (1993) 324–335.
[6] A.J. Patti, M.I. Sezan, A.M. Tekalp, Digital video standards conversion in the presence of accelerated motion, Signal Processing: Image Communication 6 (1994) 213–227.
[7] S.P. Kim, N.K. Bose, Reconstruction of 2-d bandlimited discrete signals from nonuniform samples, IEE Proceedings 137 (Pt. F3) (1990) 197–204.
[8] A. Feuer, N. Goldberg, G.C. Goodwin, Super-resolution reconstruction using spatio-temporal filtering, Journal of Visual Communication and Image Representation 14 (4) (2003) 508–525.
[9] H. Ur, D. Gross, Improved resolution from sub-pixel shifted pictures, Graphical Models and Image Processing 54 (1992) 181–186.
[10] Subhasis Chaudhuri (Ed.), Super Resolution Imaging: The Kluwer International Series in Engineering and Computer Science, Kluwer Academic Publishers, Dordrecht, 2001.
[11] Eric Dubois, The sampling and reconstruction of time-varying imagery with application in video systems, Proceedings of the IEEE 73 (4) (1985) 502–522.
[12] Sean Borman, Robert L. Stevenson, Super-resolution from image sequence – a review, Proceedings of the Midwest Symposium on Circuits and Systems (1998) 374–378.
[13] A. Feuer, G.C. Goodwin, Reconstruction of multi-dimensional bandlimited signals from nonuniform and generalized samples, IEEE Transactions on Signal Processing 53 (11) (2005) 4273–4282.
[14] K.F. Cheung, A multidimensional extension of Papoulis' generalized sampling expansion with application in minimum density sampling, in: R.J. Marks II (Ed.), Advanced Topics in Shannon Sampling and Interpolation Theory, 1993, pp. 86–119.
[15] A. Feuer, On the necessity of Papoulis result for multi-dimensional (GSE), IEEE Signal Processing Letters 11 (4) (2004) 420–422.

[16] A. Feuer, A. Allouche, G.C. Goodwin, Motion aided sampling and reconstruction, IEE Proceedings on Vision Image and Signal Processing 152 (1) (2005) 115–121.
[17] R.J. Evans, I.M. Isaacs, Generalized Vandermonde determinants and roots of unity of prime order, Proceedings of the American Mathematical Society 58 (1976) 51–54.
[18] A.M. Tekalp, Digital Video Processing, Prentice-Hall, Upper Saddle River, NJ 07458, 1995.
[19] R.A. Mollin, Fundamental Number Theory with Applications, CRC Press, New York, 1998.
[20] A.N. Netravali, B.G. Haskell, Digital Pictures: Representation, Compression and Standards, second ed., Plenum Press, New York, 1995.